Magnetic Bremsstrahlung in an Intense Magnetic Field*

C. S. Shen
Department of Physics, Purdue University, Lafayette, Indiana 47907
(Received 16 May 1972)

A number of astrophysical discoveries and laboratory developments have prompted the need to consider synchrotron emission including effects of radiation reaction and quantum corrections. In this article we first solved the Lorentz-Dirac equation to give the trajectory and radiation spectrum of a relativistic electron at strong radiation damping. The results are presented in forms which can be directly tested in experiments using megagauss magnetic fields as targets for high energy electron beams. The quantum mechanical effects which often intermingle with the classical radiation reaction effects are discussed. A quantum mechanical calculation including the effects of energy damping and quantum fluctuations is presented. The results obtained for a single electron are applied to an ensemble of electrons. The characteristics of the emission spectra are summarized in the final section for various ranges of field intensity and particle energy.

I. INTRODUCTION

A charged particle accelerated in an applied field radiates energy. In return the radiation affects the motion of the particle. Thus the dynamics and radiation of an accelerated charge particle can be summarized in Fig. 1. In Fig. 1 link 1 indicates the effect of applied field on particle motion, link 2 specifies the field produced by the particle, and link 3 represents the feedback effect on the motion of the particle by the resulting fields. Accordingly, the mathematical theory of classical electrodynamics should comprise two basic sets of equations: One, which describes the resulting fields, is represented by the Maxwell's equations; and the other, which includes the effect of both the applied field and the radiative reactions, specifies the motion of the particle. These general equations of motion should be covariant and should lead to the conservation of momentum of the field and particle; they should also reduce to the Lorentz force equations when radiation can be neglected. A partial differential equation which satisfies all three conditions was derived by Abraham, Lorentz, and Dirac,[1]

$$\dot{u}_\mu = \omega_{\mu\nu} u^\nu + \omega_0^{-1}\left(\ddot{u}_\mu - \frac{1}{c^2}\, u_\mu \dot{u}^\nu \dot{u}_\nu\right), \qquad (1)$$

where $\omega_0 = 3mc^3/2e^2 = 1.8\times 10^{23}\ \mathrm{sec}^{-1}$ is the fundamental frequency of a free electron, u_μ is the four-velocity, $\dot{u}_\mu = du_\mu/d\tau$ denotes the derivative with respect to proper time, and $\omega_{\mu\nu}$ is the electromagnetic field tensor, converted to frequency units for convenience:

$$\omega_{\mu\nu} = \frac{e}{mc}\begin{bmatrix} 0 & H_z & -H_y & E_x \\ -H_z & 0 & H_x & E_y \\ H_y & -H_x & 0 & E_z \\ -E_x & -E_y & -E_z & 0 \end{bmatrix}.$$

Equation (1) is the Lorentz-Dirac equation. It is one of the most controversial equations in the history of physics. Although all reasonable approaches seem to converge to the same expression, it does lead to many difficulties. The appearance of the third time derivative sets the equation apart from all other dynamical equations which completely specify the trajectory of a particle once the initial conditions of position and velocity are given. A natural solution of the Lorentz-Dirac equation leads to "run-away" acceleration which can be eliminated by imposing asymptotic conditions, but then the solution gives preacceleration which violates causality.

All those shortcomings have been studied extensively in the literature. Excellent reviews can be found in Rohrlich[1] and Erber.[2] It is fair to say that within the realm of classical electrodynamics the Lorentz-Dirac equation is "perhaps" the exact equation of motion for a *point charge*.[3] We say "perhaps" because the arguments leading to this equation are not without *ad hoc* flavor, and, more important, the Lorentz-Dirac equation has yet to be tested experimentally.

The purpose of this paper is not to present any further theoretical argument, pro or con, for Eq. (1) but rather to treat it as the basic cornerstone of classical electrodynamics and proceed to derive observable results for possible experimental tests. For this purpose we have chosen to analyze the

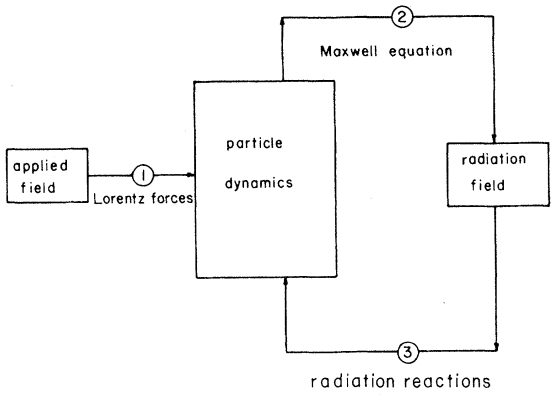

FIG. 1. Schematic diagram of the action and reaction on a classical point charge in an external field.

special case of a relativistic electron moving in a uniform, static magnetic field. The motivation behind such a choice is twofold. First, synchrotron radiation plays an extremely important role in astrophysical applications, and in many cases of current interest, such as pulsar radiation, etc. the circumstantial parameters are such that the radiative reaction forces, represented by link 3, are actually stronger than the applied Lorentz forces. Thus for a consistent treatment, one needs to have a theory including strong radiation reactions. Secondly, recent developments on the technique of flux compressions make possible the generation of transient magnetic fields up to 10 MG in the laboratory,[4-6] and electron beams of energy up to a few hundred GeV should be available soon at the National Accelerator Laboratory. As shown in Sec. III these laboratory conditions provide excellent opportunities to test experimentally the Lorentz-Dirac equation under *strong* radiative damping. A detailed calculation on high-energy magnetic bremsstrahlung is therefore timely from an experimental point of view.

We shall outline here the basic approach used in the present calculation and points of departure compared with previous treatments. It can be easily seen that the order of magnitude of the three terms on the right side of Eq. (1) is given by the ratio 1: ω_{ik}/ω_0: $\gamma^2\beta^2\omega_{ik}/\omega_0$, where $\beta = v/c$ and $\gamma = (1-\beta^2)^{-1/2}$. Thus for a highly relativistic particle the ratio of the radiation reaction force to the applied Lorentz force is given by the parameter $R_c = \gamma^2\omega_{ik}/\omega_0$, which also indicates the fractional energy loss per revolution. In the case of weak radiation damping, Eq. (1) can be expanded in powers of R_c. To the zeroth order we have

$$\dot{u}_\mu = \omega_{\mu\nu} u^\nu . \tag{2}$$

The more familiar space-time forms of Eq. (2) are

$$\frac{d\vec{p}}{dt} = e\left(\vec{E} + \frac{\vec{v}\times\vec{H}}{c}\right), \tag{2a}$$

$$\frac{dW}{dt} = e\vec{v}\cdot\vec{E} . \tag{2b}$$

Including the first-order terms we have

$$\dot{u}_\mu = \omega_{\mu\nu} u^\nu - \omega_0^{-1} c^{-2} (\omega_{\mu\nu} u^\nu)^2 u_\mu . \tag{3}$$

The spacelike component of Eq. (3) is

$$\frac{dp_i}{dt} = e\left\{E_i + \frac{v_j H_k}{c} - \frac{v_k H_j}{c} - \frac{e^2}{mc}\omega_0^{-1}\gamma^2\left[(E_j - H_k)^2 + (E_k + H_j)^2\right]\right\}, \tag{3a}$$

which includes the leading term of the damping force. The timelike component,

$$\frac{dW}{dt} = e\vec{E}\cdot\vec{v} - \frac{e^2}{m^2}\omega_0^{-1}\gamma^2\left\{\left[(\vec{\beta}\times\vec{H}) + \vec{E}\right]^2 - (\vec{E}\cdot\vec{\beta})^2\right\}, \tag{3b}$$

represents the work done by the field minus the leading terms in radiation loss. The higher-order terms in R_c can be added to Eq. (3) by successive iteration. This perturbation treatment has been utilized in the past for solving electrodynamical problems involving weak radiative damping. Plass has derived solutions to the first order in R_c for the synchrotron emissions.[7]

In Secs. II and III of the present work Eq. (1) is solved in powers of R_c/γ (and $1/\gamma$) instead of R_c. This is made possible by the transformation of Eq. (1) into the rest frame of the particle. When the applied field is solely magnetic, the ratio of the radiation-reaction term to the Lorentz-force term in the particle's rest frame is R_c/γ instead of R_c. By making this transformation we have achieved three purposes: (a) when the particle is highly relativistic, this power expansion covers cases of strong radiative damping, i.e., $F_R > F_L$; (b) the solutions obtained can be considered "exact" within the realm of classical electrodynamics, provided $\gamma \gg 137$. This statement can be explained as follows: There are two conditions restricting the applicability of classical electrodynamics. First of all, the de Broglie wavelength of the electron must be small in comparison with the minimum of the characteristic lengths. In a uniform magnetic field this length is represented by the Larmor radius $W\beta/eH$. Thus in order to treat the electron as a point charge moving in a well-defined orbit without wave interference we need

$$\gamma^2\beta^2 \gg \hbar eH/m^2c^3$$

or

$$\gamma^3\beta^2 \gg R_q ,$$

where $R_q = \frac{3}{2}\gamma H/H_q$, $H_q = m^2c^3/e\hbar = 4.4\times 10^{13}$ G. Secondly, the discrete nature of photon emission must be insignificant. In other words, the emission process should be adequately described by the classical radiation theory. A quantum mechanical treatment of synchrotron emission has been given by Klepikov and Sokolov[8] and Schwinger[8]; their results indicate that the differences between the classical and quantum mechanical calculations are characterized by the parameter R_q. Thus the classical radiation theory is an adequate approximation of the quantum radiation theory only when

$$R_q \ll 1 .$$

From the above criteria we observe that, for a relativistic electron, even though the particle itself may be a well-localized point charge, the validity of classical calculation is limited by $R_q \ll 1$. Since $R_q = \frac{9}{4}R_c(\gamma\alpha)^{-1}$, where $\alpha = e^2/\hbar c \approx 1/137$, it is justified to say that although expansion techniques are used in solving the Lorentz-Dirac equation, the solutions obtained by neglecting higher-order terms of R_c/γ are "exact" within the realm of classical electrodynamics. (c) The terms in the solution grouped in powers of R_c/γ provide physical insight into the effect of radiation reactions. The modifications due to energy damping are proportional to R_c while those due to radiative "corrections" are of the order of $(R_c/\gamma)^2$. This is consistent with the results of quantum electrodynamics.[9]

The rest of this article consists of four sections. In Sec. II we solve the Lorentz-Dirac equation to give the trajectory and the radiation spectrum of a relativistic electron at strong radiation damping. A part of the results of this section has been reported in a previous short communication to Physical Review Letters.[10] In Sec. III the mathematical results obtained in Sec. II are used to derive the deflection angle of an electron passing through a uniform magnetic field. This deflection can be measured in the experiments using megagauss field pulses as targets for NAL electron beams. In Sec. IV we compare the quantum theory of radiation reaction with that of the classical radiation reaction. A quantum mechanical calculation of the deflection angle for an electron passing through a strong magnetic field including the effects of radiation damping and quantum fluctuations is presented. In Sec. V the domains of validity of the four levels of electrodynamics, exact relativistic quantum electrodynamics, relativistic quantum electrodynamics with first-order perturbation, classical electrodynamics including radiation reaction, and classical electrodynamics without radiation reaction are discussed in terms of the field strength and the particle energy. The synchrotron radiation formulas applicable to each domain are summarized and applied to an ensemble of electrons with power-law energy distribution.

II. MATHEMATICAL ANALYSIS

Let us consider the case of a relativistic charged particle moving in a uniform static magnetic field directed along the z axis. In the Lorentz-Dirac equation the four-acceleration is given by

$$\dot{u}_\mu = \omega_{\mu\nu}u^\nu + \omega_0^{-1}\left(\ddot{u}_\mu - \frac{1}{c^2}\,u_\mu \dot{u}^\nu \dot{u}_\nu\right) . \tag{1}$$

The tensor

$$\omega_{\mu\nu} = \begin{bmatrix} 0 & \omega_H & 0 & 0 \\ -\omega_H & 0 & 0 & 0 \\ 0 & 0 & 0 & 0 \\ 0 & 0 & 0 & 0 \end{bmatrix},$$

where $\omega_H = eH/mc$. The main effect of radiation reaction is contained in the third term, $-\omega_0^{-1}c^{-2}\dot{u}^\nu\dot{u}_\nu u_\mu$, which dominates the Lorentz force when $R_c > 1$. Since $\dot{u}^\nu\dot{u}_\nu$ is a four-scalar, it must be equal to $\dot{u}^\nu\dot{u}_\nu$ in the instantaneous rest frame of the particle. In the rest frame, where the particles sees an electric field of the order γH, the ratio $(|\vec{F}_R|/|\vec{F}_L|)_{\text{rest}}$ is reduced by a factor of γ and equal to R_c/γ. Thus one can treat R_c as finite and evaluate $\dot{u}^\nu\dot{u}_\nu$ in the rest frame in powers of γ^{-1}. To the lowest order we have

$$\dot{u}'_\mu = \omega'_{\mu\nu}u'^\nu + \omega_0^{-1}\left(\omega'_{\mu\nu}\omega'_{\nu\lambda}u'^\lambda - \frac{1}{c^2}\,\omega'_{\nu\lambda}\omega'^{\nu\sigma}u'^\lambda u'_\sigma u'_\mu\right) ,$$

where u'_μ and $\omega'_{\mu\nu}$ are the four-velocity and the electromagnetic tensor in the rest frame. The dot denotes derivatives with respect to proper time.

Since $\dot{u}'_4 = 0$ in the rest frame of the particle we find

$$(\dot{u}^\nu\dot{u}_\nu)_{\text{lab}} = (\dot{u}^\nu\dot{u}_\nu)_{\text{rest}}$$
$$= \gamma^2c^2\omega_\perp{}^2\left[1 + (R_c/\gamma)^2\left(1 + \frac{2\dot{\gamma}\omega_0}{\gamma^3\omega_\perp{}^2} - \frac{\omega_0{}^2}{\gamma^4\omega_\perp{}^2}\right) + O((R_c/\gamma)^4)\right] , \tag{4}$$

where $\omega_\perp = \omega_H \sin\varphi$, and φ is the angle between the velocity $\vec{v}$ and the field $\vec{H}$. Substituting Eq. (4) into Eq. (1), we find that $\dot{u}_4$ is decoupled from the spacelike component to give the instantaneous radiation rate

$$\frac{d\gamma}{dt} = \gamma\dot{\gamma}$$

$$= \frac{-\gamma^2\omega_\perp^2}{\omega_0}\left[1 - \frac{\gamma^2\omega_\perp^2}{\omega_0^2}\left(4 + \frac{\omega_0^2}{\gamma^4\omega_\perp^2}\right)\sin^2\varphi + O\left(\left(\frac{\gamma^2\omega_\perp^2}{\omega_0^2}\right)^4\right)\right]. \tag{5}$$

Integration of Eq. (5) gives

$$\gamma(t) = \gamma_0\left\{1 + \frac{R_0\omega_\perp t}{\gamma_0[1 - 4(R_0/\gamma_0)^2(1 + R_0^{-2})/(1 + R_0\omega_\perp t/\gamma_0)]}\right\}, \tag{6}$$

where γ_0 and R_0 refer to initial values of γ and $R_c \sin\varphi$. Equation (5) and Eq. (6) differ from the standard formula which neglects radiation effects by terms of the order $(R_c/\gamma)^2$. Thus the radiative reactions modify the radiation rate only slightly. After one cycle the energy of the particle is reduced to $\sim(1 + 4\pi R_0)^{-1}$. (Since the orbit is no longer closed, "cycle" here means the particle returning to its original direction.)

Substituting Eqs. (5) and (6) into Eq. (1) gives

$$v_1 = v_0 e^{-h(t)} \cos f(t) \sin\varphi_0, \tag{7a}$$

$$v_2 = v_0 e^{-h(t)} \sin f(t) \sin\varphi_0, \tag{7b}$$

$$v_3 = v_0 \cos\varphi_0, \tag{7c}$$

where φ_0 is the angle between the velocity $\vec{v}$ and the field $\vec{H}$ at $t = 0$,

$$h(t) = \frac{R_0\omega_H t}{\gamma_0^3}\left[1 + \frac{R_0\omega_H t}{2\gamma_0} + O((R_0/\gamma_0)^2)\right] \tag{8}$$

$$f(t) = \frac{\omega_H t}{\gamma_0}\left\{\left(1 + \frac{R_0\omega_H t}{2\gamma_0}\right) - \left(\frac{R_0}{\gamma_0}\right)^2\left[\frac{6 + 2R_0^{-2}}{1 + R_0^{-2}} + \frac{R_0\omega_H t}{\gamma_0} - \frac{4\gamma_0 \ln(1 + R_0\omega_H t/\gamma_0)}{R_0\omega_H t(1 + R_0 - z)}\right]\right\}. \tag{9}$$

In Eqs. (5), (7), (8), and (9) we have retained terms proportional to $(R_c/\gamma)^2$ in order to compare them with the radiation corrections resulting from quantum mechanical calculations.

Equations (6) and (7) describe the trajectory and the energy variation of a particle under conditions of strong radiation. The trajectory is a shrinking helix (Fig. 2) with the radius of curvature $\rho(t) = v^2/(dv/dt)$ decreasing as $(1 + \gamma_0^{-1}R_0\omega_\perp t)^{-1}$. After completing the first cycle both ρ and the particle energy are reduced by a factor of $(1 + 4\pi R_0)^{-1/2}$. Two interesting points may be brought to attention:

(a) The radiative reactions modify the instantaneous energy loss rate only slightly [to the order of $(R_0/\gamma_0)^2$]. This results from the fact that forces exerted by radiative damping are mostly along the direction of $\vec{v}$ while the force exerted by the magnetic field is perpendicular to the velocity. For comparable parallel and perpendicular forces the total radiation due to the parallel component is of the order $1/\gamma^2$ smaller than that from the perpendicular component. Thus within the range of validity of classical electrodynamics radiative reaction forces cannot change the instantaneous emission rate significantly, although alterations of the orbit of the particle could be large, hence the effect on the frequency distribution of the total rad-

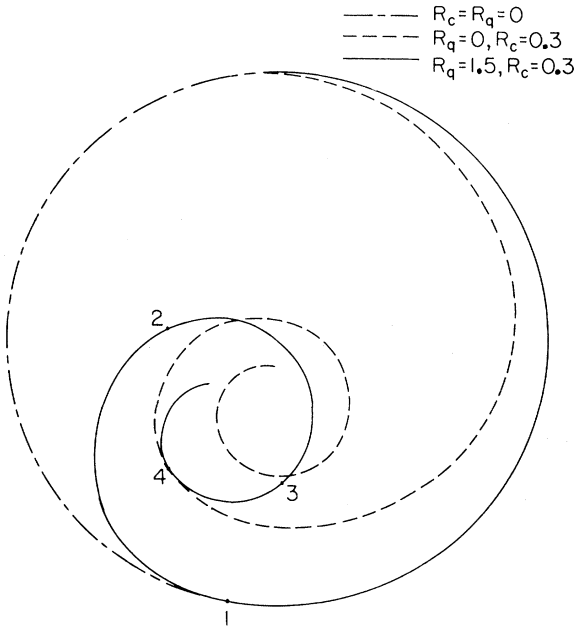

FIG. 2. Orbit of a radiating electron. Classically, the shrinking of the radius is continuous. Quantum mechanically the trajectory is composed of segments of circular arcs with successively smaller radii of curvature. The numbers 1 to 4 alongside the solid line denote the instants that a photon is being emitted.

iation may be significant.

(b) The decay rate of the angle between the velocity vector $\vec{v}$ and the field $\vec{H}$ is much slower (by a factor γ^{-2}) than the decay rate of the particle's energy. The variation of the particle's pitch angle with radiation can be best explained by Eq. (7c) which shows that the longitudinal velocity of a radiating particle is an invariant in a constant magnetic field. From Eq. (7) we have

$$\frac{dp_\perp}{dt} = p_\perp\left(\frac{d\gamma}{dt}\Big/\gamma + \frac{dv_\perp}{dt}\Big/v_\perp\right), \tag{10a}$$

$$\frac{dp_\parallel}{dt} = p_\parallel \frac{d\gamma}{dt}\Big/\gamma, \tag{10b}$$

and

$$\frac{d\gamma}{dt} = \gamma^3 v_\perp \frac{dv_\perp}{dt}\Big/c^2, \tag{11}$$

where $p_\perp = \gamma m(v_1^2 + v_2^2)^{1/2}$ and $p_\parallel = \gamma m v_3$. Combination of Eq. (10) and Eq. (11) gives

$$\frac{dp_\parallel}{dt}\Big/\frac{dp_\perp}{dt} = \frac{p_\parallel}{p_\perp}\frac{\gamma^2\beta_\perp^2}{1+\gamma^2\beta_\perp^2}. \tag{12}$$

Hence in the nonrelativistic case radiation draws all of its energy from the transverse component of motion, and the particle's pitch angle decreases with the reduction of its energy. A nonrelativistic particle injected randomly into the field would lose about $\frac{2}{3}$ of its initial energy, then stream along the field line with no further radiation losses. But this is not true for a relativistic particle. For $\gamma \gg 1$ the ratio of the longitudinal energy loss to the transverse energy loss is equal to the ratio of the initial values of the two respective components. Although the particle's radius of gyration and its energy decrease quickly at strong radiative damping, the *pitch angle remains practically constant.*[11]

Derivation of the results of this section and those that follow involve Lorentz transformations between the instantaneous rest frame and the laboratory frame. Since the particle at strong radiative damping is under enormous acceleration, one might question the validity of such transformations.[12] However, the instantaneous rest frame considered here is not a frame attached to the particle. It is a frame which moves with a (uniform) velocity equal, in magnitude and direction, to the velocity of the particle at the instant of consideration. The particle, although motionless (or nearly motionless if an infinitesimal time apart from the instant), is under acceleration in this instantaneous rest frame. This is by definition an inertial frame irrespective of the magnitude of the acceleration, and the Lorentz transformations used here are strictly valid. Such a choice of coordinates is effective only when the consideration is limited to the motion of the particle as a whole. If the particle possesses internal structure (spin, for example) and one wants to study the effect of external field on these internal properties, then the equation of motion describing the change of these properties must be expressed in a frame attached to the particle. This frame, which rotates with respect to the instantaneous rest frame by an angular velocity

$$\vec{\omega}_T = (\gamma - 1)\left(\vec{v}\times\frac{d\vec{v}'}{dt}\right)v^{-2},$$

is of course not an inertial frame. This effect leads to the famous example of Thomas precession. For the synchrotron problem the computations become unnecessarily complicated if one wants to carry them out in the particle's frame. Still, it can be easily shown that

$$\left(\frac{d\vec{v}}{dt}\right)_{\text{particle's frame}} = \left(\frac{d\vec{v}}{dt}\right)_{\text{instantaneous inertial frame}} \times[1+O(1/\gamma)]; \tag{13}$$

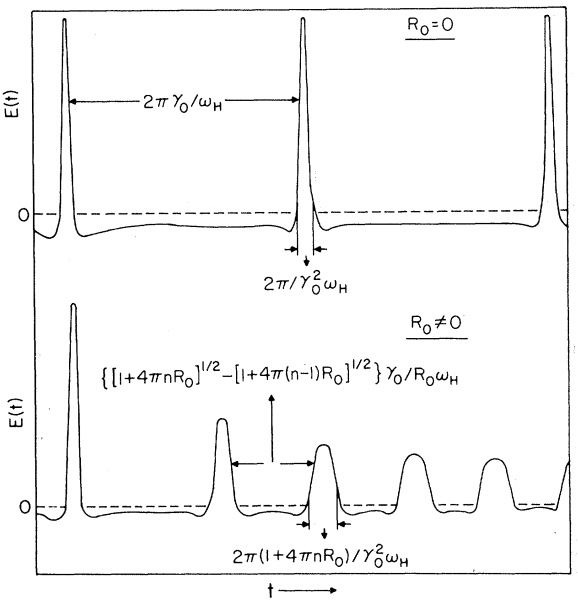

FIG. 3. Schematic drawing of the radiation field impinging on a distant observer for electrons moving in a magnetic field. (a) represents the field without radiation damping; (b) represents the field with radiation damping, where the intensity and the time interval between successive pulses decrease but the duration of each pulse increases.

thus no practical difference results from the intermediate steps.

The spectrum of synchrotron radiation of a particle at strong radiation damping can be derived from Eqs. (5) and (7). It is well known that radiation emitted by a relativistic particle is concentrated in the forward direction of motion.[13,14] Since the trajectory of a charged particle in a homogeneous magnetic field is a spiral along the direction of $\vec{H}$, a distant recording device (the observer) will receive successive pulses of radiation at those moments when the particle is moving toward him. In ordinary synchrotron emission, where the effect of radiation reaction on the particle is neglected, the bursts will be repeated at a constant time interval $\Delta T \approx \gamma\omega_H^{-1}$. The characteristics of each burst, which have a duration of the order of $\Delta t \approx (\gamma^2\omega_H)^{-1}$, are identical; thus the observer will record a field shown schematically by the curve in Fig. 3(a). The Fourier spectrum of the field is discrete, consisting of harmonics of the fundamental frequency $(\Delta T)^{-1} = \omega_H/\gamma$.

Since $\Delta T/\Delta t \approx \gamma^3 \gg 1$, the characteristics of the "instantaneous spectrum," representing the spectrum of a single burst, are given by

$$\left.\frac{dI(\omega)}{d\Omega}\right|_{\text{inst}} = \frac{e^2\omega^2}{4\pi^2c^3}\left|\int_{-\Delta T/2}^{\Delta T/2} \vec{n}\times(\vec{n}\times\vec{v})e^{i\omega(t-\vec{n}\cdot\vec{r}/c)}dt\right|^2 . \tag{14}$$

The observed radiation consists of many bursts,

$$\left.\frac{dI(\omega)}{d\Omega}\right|_{\text{obs}} = \sum_{n=1}^{\infty}\left.\frac{dI(\omega)}{d\Omega}\right|_{\omega=n\omega_H/\gamma} . \tag{15}$$

However, the case is different at strong radiative damping. The orbit of the particle is no longer periodic. The time intervals between successive pulses, as well as the character of each pulse, are not the same. This is shown schematically in Fig. 3(b). The "instantaneous spectrum," which represents a particular pulse, and the "cumulative spectrum," which represents the Fourier transform of a number of successive bursts, are not the same. In most astrophysical cases where the observation time is much longer than the repetition interval ΔT, the cumulative spectrum is what one would see. On the other hand, in certain laboratory experiments, such as the one we shall discuss in the next section, the recording device will receive only one burst when the searchlight beam emitted by the deflected electron sweeps across the observer. We shall discuss the two spectra separately. *(a) Instantaneous Spectrum.* We shall assume that both the observation time and the time for which the acceleration differs from zero are much longer than the duration of the pulse. Then the radiation spectrum is related to its trajectory by[13]

$$\frac{dI(\omega)}{d\Omega} = \frac{e^2\omega^2}{4\pi^2c^3}\left|\int_{-\infty}^{\infty} \vec{n}\times(\vec{n}\times\vec{v})e^{i\omega(t-\vec{n}\cdot\vec{r}/c)}\,dt\right|^2 . \tag{16}$$

We note that the integration is to be performed in the particle's own time, where the duration of the pulse is $\sim\omega_H^{-1}$. Thus $\vec{v}$ and $\vec{r}$, given by Eq. (7), can be expanded in powers of $1/\gamma_0$, R_0/γ_0, and $\omega_H t/\gamma_0$ in the integrand of Eq. (16), and the integration can be carried out to express the radiation spectrum in terms of parabolic cylindrical functions. Intensity, polarization, and shape of the spectrum are all modified slightly, to the order of (R_0/γ_0), as compared with the synchrotron spectrum neglecting radiative damping. This is consistent with the result obtained in the previous section that the radiation rate itself is modified only slightly by radiation. A more detailed discussion and derivation of the spectrum are given in Appendix A. *(b) Cumulative Spectrum.* For most cases the observation time is much longer than the period of revolution of the charged particle; then the recording device will receive successive pulses at those moments when the particle is moving toward it. Let us consider an observer located on the x axis and the particle moving in the x-y plane. From Eq. (6) we see that he receives bursts of radiation when $v_2(t) = 0$, or at

$$t = t_n = \left[\frac{(1+4\pi nR_0)^{1/2}-1}{R_0}\right]\frac{\gamma_0}{\omega_H} , \tag{17}$$

while the energy of the emitting particle is $\gamma(t_n) = \gamma_n = \gamma_0(1+4\pi nR_0)^{-1/2}$. The observer records a series of closely bunched pulses. The time interval between successive pulses decreases while the duration of each pulse increases. The total radiation from the particle is the superposition of all pulses. Therefore the radiation spectrum may be expressed as

$$\frac{dI(\omega)}{d\Omega} = \frac{e^2\omega^2}{4\pi^2c^3}\left|\int_{-\infty}^{\infty} \vec{n}\times(\vec{n}\times\vec{v})e^{i\omega(t-\vec{n}\cdot\vec{r}/c)}\,dt\right|^2$$
$$= \frac{e^2\omega^2}{4\pi^2c^3}\left|\sum_{n=0}^{N}\int_{(t_{n-1}+t_n)/2}^{(t_n+t_{n+1})/2} \vec{n}\times(\vec{n}\times\vec{v})e^{i\omega(t-\vec{n}\cdot\vec{r}/c)}\,dt\right|^2 . \tag{18}$$

The lower limit of the summation corresponds to the time the particle is injected into the emission region, which is taken to be $t=0$. The upper limit of the summation corresponds to the observation period T (or the time the emitting particle stayed in the observation region, if it is shorter than T). From Eq. (17)

$$N=\frac{\omega_H T}{2\pi\gamma_0}\left(1+\frac{R_0\omega_H T}{2\gamma_0}\right). \tag{19}$$

The nth term in the summation represents the Fourier transform of the amplitude of the nth pulse. Since the radiation of each pulse is concentrated within a time interval $(\gamma_n^2\omega_H)^{-1}$ around t_n where the duration between successive pulses is $\gamma_n\omega_H^{-1}$, the limits of integration for each term in the summation can be replaced by $\pm\infty$ after a suitable transformation of variables. With this approximation, Eq. (6) can be evaluated following the usual procedure of computing the radiation spectrum from an ultrarelativistic particle,

$$\frac{dI(\omega)}{d\Omega}=\frac{e^2\omega^2}{3\pi^2 c\gamma_0^2\omega_H^2}\left[A_{\parallel}^2(\omega)+A_{\perp}^2(\omega)\right]. \tag{20}$$

$A_{\parallel}^2(\omega)$ and $A_{\perp}^2(\omega)$ correspond to the two polarization components,

$$A_{\parallel}^2(\omega)=\sum_{n=0}^{N} a_n^2(\theta)b_n^{-1}\left[K_{2/3}^2\left(\frac{\omega}{\omega_n}\right)+\left(\frac{R_0}{\gamma_0}\right)^2 a_n^{-1}(\theta)K_{1/3}^2\left(\frac{\omega}{\omega_n}\right)\right], \tag{21a}$$

$$A_{\perp}^2(\omega)=\sum_{n=0}^{N} a_n(\theta)b_n^{-1}\gamma_0^2\theta^2K_{1/3}^2\left(\frac{\omega}{\omega_n}\right), \tag{21b}$$

where

$$\begin{aligned} a_n(\theta)&=1+\gamma_0^2\theta^2+4\pi nR_0,\\ b_n&=1+4\pi nR_0,\\ \omega_n&=3\gamma_0^2\omega_H b_n^{1/2}\left[a_n(\theta)-R_0^2/\gamma_0^2\right]^{-3/2}, \end{aligned} \tag{22}$$

and θ is the colatitude angle the observer makes with the orbiting plane. $K_{2/3}$ and $K_{1/3}$ are modified Bessel functions. In Eq. (21) the differences between the spectrum of an individual pulse and the classical expression for radiation emitted by a relativistic particle of energy γ_n and radius of curvature ρ_n are of the order of $(R_n/\gamma_n)^2$, a result consistent with that obtained in the Appendix.

All information about the radiation is contained in Eq. (7). Of particular interest for astrophysical applications are the polarization and frequency distribution of radiation. The frequency distribution of the total energy emitted by a particle of initial energy γ_0 is

$$\begin{aligned} I(\gamma_0,\omega)&=\int\frac{dI(\omega)}{d\Omega}\,d\Omega\\ &=\frac{2e^2\omega}{\sqrt{3}\,c\gamma_0\omega_H}\sum_{n=0}^{N} b_n\int_{2b_nN^2\omega/3\gamma_0^2\omega_H}^{\infty}K_{5/3}(x)dx+O\left(\left(\frac{R_0}{\gamma_0}\right)^2\right) \end{aligned} \tag{23}$$

$I(\gamma_0,\omega)$ is plotted in Fig. 4 for $R_0=10^{-2}$ and 10. In the high-frequency range $\xi=\omega/\gamma_0^2\omega_H>(1+4\pi R_0)^{-1}$ the spectrum varies as $\xi^{1/2}e^{-2\xi/3}$. In the intermediate range

$$(1+R_0\omega_H T/\gamma_0)^{-2}<\xi<(1+4\pi R_0)^{-1}$$

the spectrum varies as $\xi^{-1/2}$; in the very low-frequency range $\xi<(1+R_0\omega_H T/\gamma_0)^{-2}$ the spectrum varies as $\xi^{1/3}$. The polarization of the radiation is given by

$$\Pi(\omega)=\frac{A_{\parallel}^2(\omega)-A_{\perp}^2(\omega)}{A_{\parallel}^2(\omega)+A_{\perp}^2(\omega)}. \tag{24}$$

The values of $\Pi(\omega)$ are plotted in Fig. 5 for the same sets of parameters as $I(\omega)$. In the frequency range of $(1+4\pi R_0)^{-1/2}\gg\xi\gg\xi_f$, $\Pi(\omega)$ had the common value of 0.695 for all values of R. At $\xi\ll\xi_f$, Π drops to 0.5.

The results obtained above are easily generalized to cover the case that the particle's longitudinal velocity $v_3\neq 0$. One need only replace H by $H\sin\varphi_0$ in all computations. In addition $I(\gamma_0,\omega)$ should be divided by $\sin^2\varphi_0$ to take care of the Doppler effect on t_n, the interval between pulses.[15]

Equation (19) and Eq. (24) are obtained by formal derivation and give exact expressions for the spectrum and the polarization of radiation (within the prescribed conditions $R_c/\gamma\ll 1$ and $\gamma^{-1}\ll 1$). These complex results can be better understood through a qualitative explanation: Within the observation time T the observer records N pulses.

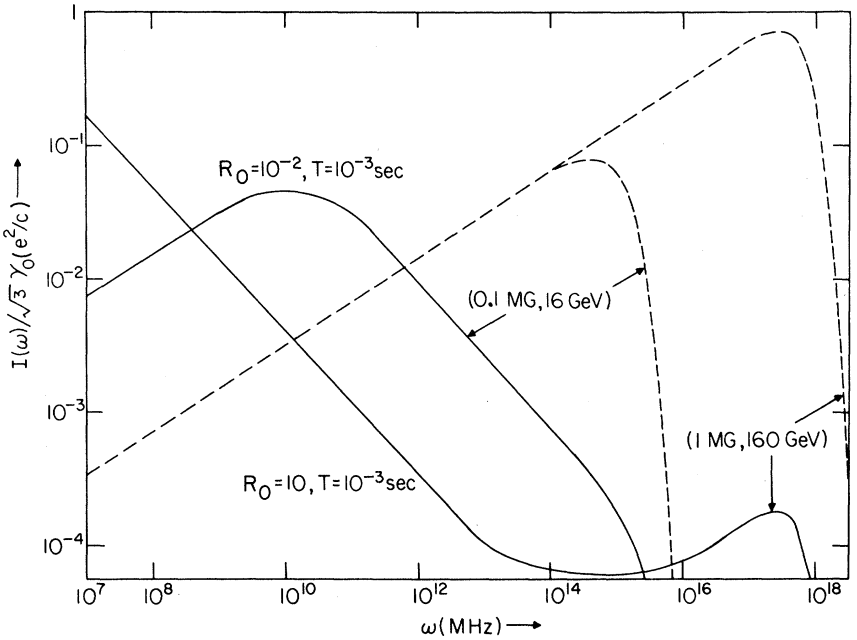

FIG. 4. The frequency spectrum of synchrotron radiation. The dashed curves are the instantaneous radiation spectra, which deviate very little from the conventional synchrotron spectrum. The solid curves are the cumulative spectrum with obvious radiation damping effect. The first maximum, which is due to the cutoff of the observation time, occurs at $\omega_0^2/\omega_H^3T^2$, while the second maximum which appears when $R_c \gtrsim 1$ occurs at $\sim\gamma_0^2\omega_H$.

Since to the lowest order of R_c/γ radiation reactions do not alter the instantaneous emission spectrum, the spectrum of each pulse is practically identical to the classical expression given by a particle of energy γ_n. Superposition of these N spectra yields the described result. For example, the frequency distribution of the instantaneous radiation emitted by an extremely relativistic particle of energy γ increases as $\omega^{1/3}$ for $\omega \ll \gamma^2\omega_H$; it reaches a maximum at $\sim 0.3\gamma^2\omega_H$ and for $\omega \gg \gamma^2\omega_H$ the intensity drops as $\omega^{1/2}e^{-(2\omega/3\gamma^2\omega_H)}$. The first pulse, therefore, gives a broad, slowly increasing spectrum cut off at $\sim\gamma_0^2\omega_H$. The second pulse, which is emitted by the particle at energy

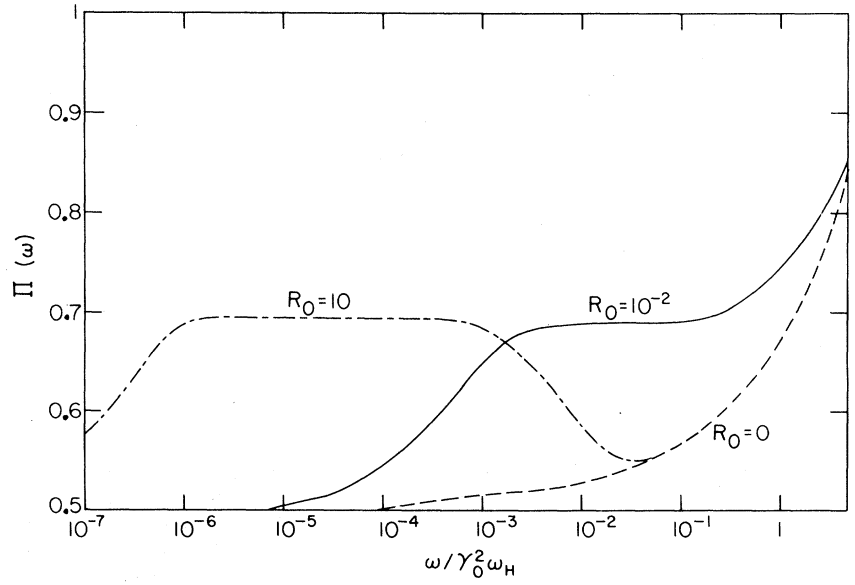

FIG. 5. Polarization of synchrotron radiation from a single electron.

$\gamma_0/(1+4\pi R_0)^{1/2}$, shows a similar spectrum but with less intensity and cut off at $\sim\gamma_0^2\omega_H/(1+4\pi R_0)$. By the same reasoning, the third and later pulses cut off at $\omega=\gamma_0^2\omega_H/(1+4\pi nR_0)$. Similarly the Nth pulse, whose intensity has been reduced vastly by a factor of

$$(1+4\pi NR_0)^{-1}\approx(1+R_0\omega_H T/\gamma_0)^{-2},$$

has a cutoff frequency at $\sim\gamma_0^2\omega_H(1+R_0\omega_H T/\gamma_0)^{-2}$. Therefore, in the frequency range $\omega>\gamma_0^2\omega_H/(1+4\pi R_0)$ only the first pulse contributes significantly to the superimposed spectrum, and its shape retains the classical form. At frequencies below $\gamma_0^2\omega_H/(1+4\pi R_0)$ the subsequent pulses join forces, one by one, and the intensity, instead of decreasing, increases toward smaller ω. If the radiation damping is strong enough, i.e., $R_0>1$, so that the first two $\omega_{\max}$'s are well apart, the spectrum will show a dip at around $\gamma_0^2\omega_H/(1+4\pi R_0)$ At the lower end of the frequency spectrum, because the observation period is finite, pulses emitted later than T will not be received, and the spectral shape at

$$\omega<\gamma_0^2\omega_H(1+R_0\omega_H T/\gamma_0)^{-2}$$

will again retain its classical form and vary as $\omega^{1/3}$. The angular distribution and polarization of the radiation can all be described similarly.

III. EXPERIMENTAL TEST

The strength of magnetic fields in electron synchrotrons is of the order of 10^4 gauss where the maximum energy of the particle attained is ~10 GeV. The damping parameter R_c is less than 10^{-3}, hence it would be very hard to study the effect of radiation damping in the existing accelerators. However, recent developments in the technique of flux compression have generated transient magnetic fields up to 10 megagauss in the laboratory with a lifetime of the order of 1 μsec.[4-6] Also secondary electron beams of energy up to a few hundred GeV should be available soon from NAL. One can readily see that these parameters yield $R_c\gtrsim 100$. For the first time, then, it appears that the classical Lorentz-Dirac equation can be subjected to experimental test by the combination of high-energy accelerators and megagauss targets.[16] A series of such experiments, using megagauss pulses as targets for high-energy electron beams (abbreviated as MPEB hereafter), have already been carried out by Erber, Herlach, Murray and Heckman at SLAC.[4,17]

The schematic of the setup of that experiment is shown in Fig. 6. The radiation and the deflection of the electron beam are measured by x-ray film and nuclear emulsions located downstream of the MG target. Of the radiative reaction effects discussed above, the one most likely to be detected is the additional deflection caused by the radiation damping. From Eq. (7) we observe that the deflection of the electron after traversing a distance L in a magnetic field is

$$\theta=f(T)=\left(1+\frac{R_0\omega_H L}{2\gamma_0 c}\right)\frac{\omega_H L}{\gamma_0 c}. \tag{25}$$

That is, in addition to the normal deflection (without radiation)

$$\theta_0=\frac{\omega_H L}{\gamma_0 c}=\frac{eHL}{E}, \tag{26}$$

there is a radiation-reaction-induced deflection

$$\delta\theta_c=\frac{R_c}{2}\left(\frac{\omega_H L}{\gamma_0 c}\right)^2=\frac{e^5H^3L^2}{3m^4c^8}. \tag{27}$$

This additional shift corresponds to the shrinking of the orbit of the particle. A useful parameter which indicates the chance of being measurable is

$$\frac{\delta\theta_c}{\theta_0}=\frac{R_c}{2}\,\theta_0=\frac{1}{3}\,\frac{e^4H^2LE}{m^4c^8}. \tag{28}$$

θ_0 and $\delta\theta_c/\theta_0$ are given in Table I in units of radian for three sets of experimental parameters. The first set, which corresponds to the SLAC experiment already carried out by the IIT group,[4] predicts a $\delta\theta_c/\theta_0$ which, in view of the experimental uncertainties, is too small to be significant. The next two sets, which correspond to the energy of the NAL beams predict fractional shifts larger than 10%. They should be measurable.

An interesting feature of the deflection angle is that the magnitude of the radiation reaction induced $\delta\theta_c$ is inversely proportional to the 4th power of the mass of the particle, where the normal deflection is a function of energy only. Thus

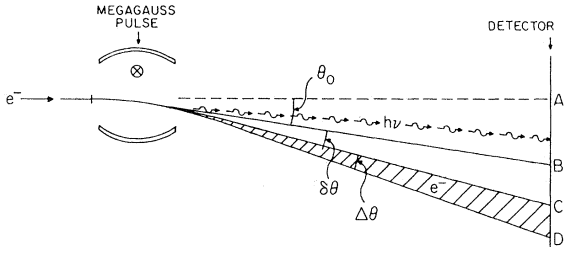

FIG. 6. Schematic diagram of the magnetic-pulse-electron-beam experiment designed by the IIT group. θ_0 is the "normal" deflection of the electron beam neglecting radiation reaction and quantum effects. $\delta\theta$ is the increment due to radiation reaction, $\Delta\theta$ is the quantum spread caused by the cascade emissions.

TABLE I. Numerical estimation on the radiation-reaction corrections. The first three columns represent experimental conditions. $\langle E_f \rangle$ is the average outgoing energy of the electrons. $\langle \theta \rangle$ is the average deflection angle. $\delta\theta_c$ and $\Delta\theta$ are, respectively, the shift due to classical radiation damping and the width due to quantum fluctuations, respectively.

E (GeV)	H (MG)	L (cm)	R_c	R_q	$\langle E_f \rangle$ (GeV)	$\langle \theta \rangle$ (rad)	$\delta\theta_c/\langle\theta\rangle$	$\Delta\theta/\langle\theta\rangle$
19	1.9	0.5	0.29	2.4×10^{-3}	18.9	1.5×10^{-2}	2.2×10^{-3}	3.2×10^{-3}
500	1	0.5	107	3.4×10^{-2}	485	3×10^{-4}	1.6×10^{-2}	3.2×10^{-2}
400	5	0.5	304	1.3×10^{-1}	369	1.9×10^{-3}	2.2×10^{-1}	8.8×10^{-2}

a beam of μ^-, say, sent through the magnetic pulse simultaneously with an electron beam of similar energy can serve the purpose of calibration. In that case one need not know the accurate value of the field strength H and the path length L, so long as one can insure adequate space-time synchronization of the two beams with the megagauss pulse. The separation between the two spots which represents the deflected μ^- beam and e^- beam, respectively, on the recording film placed downstream from the megagauss target directly gives the radiative-reaction-induced deflections. To achieve this purpose, however, the energy variation of the incoming beam must be small enough so that the angular dispersion will be smaller than the radiation-induced deflection.

In addition to the deflections, one can also measure the energy and the radiation spectrum of the emerging electrons. The energies of the emerging electrons are given by Eq. (6), with t replaced by L/C. They are listed in column 6 of Table I. The instantaneous radiation spectrum is not affected by the radiative damping, therefore the photon detector mounted downstream from the megagauss target would record a classical synchrotron spectrum with critical frequency $\omega_f = \gamma_f{}^2\omega_H$, where γ_f is the instantaneous energy of the electron at the time of emission.

IV. QUANTUM MECHANICAL RADIATION REACTION AND ITS ANALOGY WITH CLASSICAL RADIATION REACTION

In analogy to the classical electrodynamics the quantum theory of radiation can be summarized by the diagram in Fig. 7.

The present quantum theory of synchrotron emission was developed following the general perturbation method.[18] The interaction of the electron with its own virtual-photon field provides the mechanism for spontaneous emissions, but the interaction Hamiltonian H_I is treated as a small perturbation in the Dirac wave equation

$$i\hbar\frac{\partial}{\partial t}\psi = (H_0 + H_I)\psi, \tag{29}$$

where $H_0 = H_{\rm rad} + H_e$ consists of Hamiltonians representing the radiation field and an electron in the stationary magnetic field. First one solves

$$i\hbar\frac{\partial}{\partial t}\psi = H_0\psi$$

to find the unperturbed wave function for the electron and the radiation field. The eigenstates of H_e are degenerate, the energy depends only on the total quantum number n,

$$E_n = mc^2\left[1 + (P_3/mc)^2 + 2nH/H_q\right]^{1/2}. \tag{30}$$

The transition probability between two unperturbed energy levels, after summing over the degenerate states, is

$$\lambda_{ij} = \frac{\alpha\omega_H}{\sqrt{3}\pi}\frac{(mc^2)^3}{E_i{}^2E_j}f(y), \tag{31}$$

where

$$f(y) = \int_y^\infty K_{5/3}(x)dx + R_q{}^2y^2(1+R_qy)^{-1}K_{2/3}(y),$$

$$y = (E_i - E_j)/R_{qi}E_j,$$

and

$$R_{qi} = \tfrac{3}{2}\gamma_iH/H_q.$$

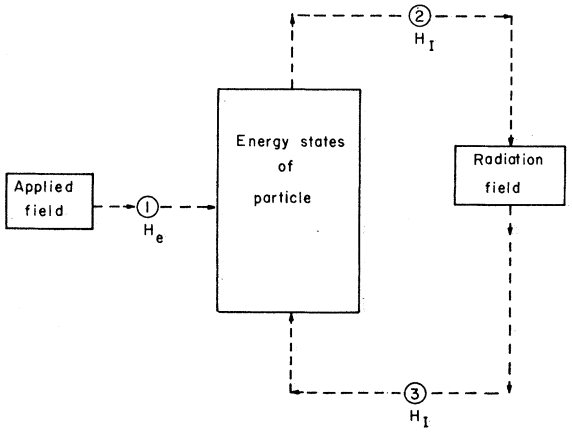

FIG. 7. Quantum mechanical description of the action and reaction on a charge in an external field.

The transition rate λ_{ij} varies as $y^{-2/3}$ for $y \ll 1$ and drops off exponentially for $y \gg 1$. The radiation spectrum of an electron at energy E_i is given by

$$\sum_j \hbar\omega_{ij}\lambda_{ij}\,,$$

$$I_i(\omega)d\omega = \frac{3\sqrt{3}}{4\pi}\, c\gamma_i^2 H^2 \left(\frac{e^2}{mc^2}\right)^2 \frac{z^2}{(1+R_{qi}z)^3} \times f(z)\,\frac{d\omega}{\omega(1-\hbar\omega/\gamma_i mc^2)}, \tag{32}$$

where $z = \hbar\omega/R_{qi}(E_i - \hbar\omega)$.

Integration of $I_i(\omega)$ over ω gives the radiation rate

$$\left(\frac{d\gamma}{dt}\right)_q = -\frac{\gamma^2\omega_H^{\,2}}{\omega_0} F(R_q), \tag{33}$$

where

$$F(R_q) = \frac{9\sqrt{3}}{8\pi}\int_0^\infty \frac{yf(y)}{(1+R_q y)^3}\,dy = 1 - 3.9R_q + 21.3R_q^{\,2}, \quad R_q \ll 1 = 1.2R_q^{-4/3}, \quad R_q \gg 1. \tag{34}$$

Equations (31) and (33) are the instantaneous radiation spectrum and the instantaneous radiation rate in quantum electrodynamics. Since in this first-order theory the wave function of the electron is derived without interference by the interaction Hamiltonian, the radiation reaction indicated by the feedback line (3) of Fig. 7 is not included. In this sense the first-order theory is the quantum mechanical analogy of the classical "reaction-less" radiation theory. The modifications characterized by R_q are due to the use of quantum mechanical calculation in processes represented by links (1) and (2).

A self-consistent treatment including the feedback loop (3) would be to solve Eq. (29) without approximations. As is well known, no exact solution has ever been found for the Dirac equation including radiations. To estimate the effect of radiation reaction one can separate the reaction effect into two parts. One part includes the modification of the total Hamiltonian due to the interactions, which we shall call "radiative corrections" (which, for example, is the cause of the well-known Lamb shift). The other part includes the damping effect due to the emission of photons. The radiative corrections are usually estimated from the higher-order terms in the expansion of H_I. For relativistic electrons in an intense magnetic field, the leading terms of the various secondary effects are proportional to αR_q for $R_q > 1$. Thus we may conclude that the validity of the first-order theory is limited to $\alpha R_q \ll 1$.[19]

Although the calculation of radiative "corrections" involves great mathematical complication, the second part of radiation reaction, the energy damping effect due to the emission of photons, can be derived exactly in a cascade calculation. This point can be best explained by comparing the physical meaning of radiation reaction in the quantum mechanical calculation and that in the classical calculation. In classical electrodynamics an accelerated particle losses energy *continuously*, thus both the damping of the particle's energy and the modification of the radiation process due to the radiation reaction are contained in the feedback loop (3) of Fig. 1. Neglecting the reaction force

$$\omega_0^{-1}\left(\ddot{u}_i - \frac{1}{c^2}\,\dot{u}^k\dot{u}_k\,u_i\right) \tag{35}$$

in the Lorentz-Dirac equation would make the radiating electron moving with constant energy, violating the energy conservation law. In the quantum mechanical treatment, the radiation consists of discrete steps. A particle stays in a state for a finite time before making a transition to a lower state. Since the lifetime in a given energy state is very short [$\tau \approx (\alpha\omega_H)^{-1}$], a particle usually makes a number of transitions during the time of observation. If one follows the transitions step by step, i.e., after the first emission, the emitted photon energy is subtracted from the initial electron energy, and the reduced energy is used in the calculation of the second emission process, and so on, then the final results will automatically include the damping effect. Such a cascade calculation has been carried out by Shen and White, and the results were presented in an earlier article.[20] In addition to the inclusion of the effect of radiation damping, a statistical phenomenon due to the discrete nature of quantum transitions appears. Under certain conditions the broadening in energy states due to statistical fluctuations may reach a magnitude comparable to the shift caused by the radiation damping. We shall estimate its effect here.

Let $\rho(E, t)$ be the number of electrons in the states within the energy range E and $E+dE$. We have

$$\frac{\partial\rho(E,t)}{\partial t} = -\frac{1}{\tau(E)}\rho(E,t) + \int_0^\infty \lambda(E,E')\rho(E',t)dE'. \tag{36}$$

Equation (36) was solved together with Eq. (31) by a straightforward numerical method in Ref. (20). The solution $\rho(E,t)$ describes the energy distribu-

tion of the particles at time t with initial distribution $\rho(E, 0)$. Observables such as the expected instantaneous radiation spectrum can be readily calculated from $\rho(E,t)$ by

$$I(\omega, t) = \int \rho(E, t) I(\omega, E) dE .$$

In Fig. 8 we have plotted $\rho(E)$ for a monochromatic incident beam after traversing various distances in H. The spread in energy states is analogous to the energy straggling which occurs when a fast particle travels through a thickness of matter. The only difference is that in ordinary bremsstrahlung the emission of a hard quantum which carries away energy comparable to that of the electron is almost equally probable as the emission of soft photons, hence the spread is insensitive to the energy of electron. In synchrotron emission the maximum fractional energy carried away by an individual quantum is characterized by $R_q(1+R_q)^{-1}$ [see Eq. (31)]; thus the straggling effect is appreciable only when R_q is not negligibly small.

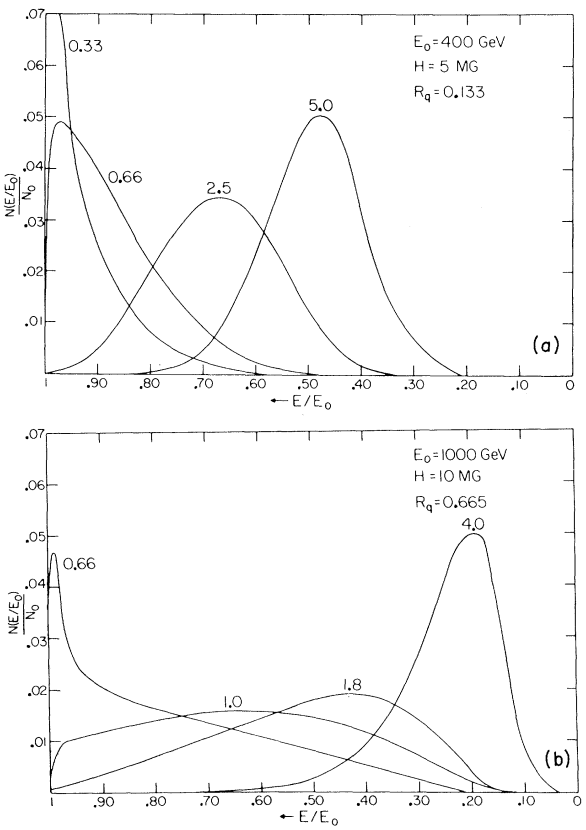

FIG. 8. Energy spectrum of a beam of monoenergetic electrons after passing through the magnetic field. The numbers affixed to the curves are the magnetopath length LH in units of cm MG. The classical energy [given by Eq. (6)] and the expected quantum mechanical energy (obtained by averaging over the distribution) are, respectively, $\gamma_c/\gamma_0 = 0.92$, 0.86, 0.61, and 0.44 and $\langle\gamma_q\rangle/\gamma_0 = 0.95$, 0.90, 0.68, and 0.50 for the four curves in (a) and $\gamma_c/\gamma_0 = 0.55$, 0.41, 0.31, and 0.16 and $x\langle\gamma_q\rangle/\gamma_0 = 0.77$, 0.65, 0.51, and 0.25 for the four curves in (b). (This figure is adopted from Shen and White, Ref. 20.)

To illustrate the relative magnitude of the fluctuation effect and the damping effect, we present a quantum mechanical calculation on the deflection angle of an electron traversing through a strong magnetic field. The rate of change of direction for a particle in the eigenstate (N_i, S_i) (N_i is the principal quantum number, which determines the energy and the radius of curvature, and S_i is the radial quantum number, which characterizes the position of the center of the trajectory) is

$$\frac{d\theta_i}{dt} = \frac{v}{r(N_i, S_i)} , \tag{37}$$

where

$$r(N_i, S_i) = \langle \psi_{N_i, S_i} | r | \psi_{N_i, S_i} \rangle$$
$$= N_i^{1/2} r_H [1 + (S_i + \tfrac{1}{2})/4N_i] , \tag{38}$$

and $r_H = (2H_q/H)^{1/2}\hbar/mc$ is the "Bohr radius" of an electron in a magnetic field. The total deflection of the electron after traversing a distance L in a magnetic field H is

$$\theta = \sum_{i=1}^{m} \frac{(t_i - t_{i-1})v}{r(N_i - S_i)} , \tag{39}$$

where t_i is the instant the particle makes the transition from state (N_i, S_i) to state (N_{i+1}, S_{i+1}), t_0 is the time the particle enters the field, and $t_m = L/c$ is the time the particle leaves the field. The duration $(t_i - t_{i-1})$, which is the length of time the particle stays in the ith state, and the probability that it will decay to the $i+1$ state are both governed by the transition probability $\lambda_{N_i, S_i, N_{i+1}, S_{i+1}}$. To evaluate θ let us first consider the factor $(S_i + \frac{1}{2})/4N_i$ in Eq. (38). As had been shown by Sokolov and Ternov[18] and Urban and Wittmann[21] the quantum member S_i is an increasing function of time

$$\frac{\Delta S_i}{\Delta t} = \int \sum_j (S_j - S_i) \lambda_{N_i, S_i, N_j, S_j} dN_j$$
$$= \frac{55}{48\sqrt{3}} \gamma^4 e^4 H^2/m^3c^5 . \tag{40}$$

Because the radiation process does not involve the change of the radial quantum number, S increases linearly with time irrespective of the level transitions. (This effect is the cause of betatron oscillations in accelerators.) After traversing a distance L_i,

$$\frac{S(L_i)}{4N_i} = \frac{S(0)}{4N_i} + \frac{55}{216\sqrt{3}}\,\alpha R_q^{\,2}\,\frac{L_i}{\lambda}\,\frac{H}{H_q}$$

$$\approx \frac{S(0)}{4N_i} + 10^{-8}H^3E^2L_i\,, \tag{41}$$

with H in MG, E in GeV, and L_i in cm. (We shall use these units of magnetic field, energy, and length for all equations in the remainder of this section.

If we choose the coordinates such that the center of the orbit coincides with the origin when the electron enters the field, and the S-dependent fluctuation correction

$$\delta_S = \frac{55}{216\sqrt{3}}\,\alpha R_q^{\,2}\,\frac{L}{\lambda}\,\frac{H}{H_q}$$

is small compared to unity, the total deflection may be expressed by

$$\theta = \theta_m(1-\delta_S), \tag{42}$$

where

$$\theta_m = \sum_{i=1}^{m} \frac{v(t_i - t_{i-1})}{N_i^{1/2}\gamma_H}\,. \tag{43}$$

θ_m can be calculated by the Monte Carlo method.[22] The distribution of the deflection angles for a beam of monochromatic energy electrons after traversing a distance in H is shown in Fig. 9. For $R_q \ll 1$, an adequate formula for $\langle\theta\rangle$, the average quantum mechanical deflection angle is

$$\langle\theta\rangle \simeq \left[1 + \frac{R_c e H_L}{2E_0}\,(1 - 4R_q + 21\,R_q^{\,2})\right]\frac{eHL}{E_0}\,. \tag{44}$$

The angular spread of the particles due to quantum fluctuation may be estimated by the mean deviation $\Delta\theta = [\langle\theta^2\rangle - \langle\theta\rangle^2]^{1/2}$. Since Eq. (43) contains two sets of restrained random variables, an approximate formula for the spread is

$$\Delta\theta \cong \frac{2}{\sqrt{\zeta}}\left(1 - \frac{\gamma(L)}{\gamma_0}\right)\langle\theta\rangle$$

$$\cong \frac{3\times10^{-5}H^{5/2}L^{3/2}}{1 + 1.3\times10^{-4}H^2LE_0}\,, \tag{45}$$

where

$$\zeta = \frac{5\alpha LH}{2\sqrt{3}\,\lambda H_q}$$

is the average number of photons emitted within L (i.e., the number of steps taken in the random cascade). Equation (45) checks well with the numerical result obtained from Monte Carlo calculations.

The total deflection may be written as

$$\langle\theta\rangle = \frac{eHL}{E_0} + \frac{e^5H^3L^2}{3m^4c^8}\,(1 - 4R_q + 21R_q^{\,2})(1-\delta_S) \tag{46}$$

with a "width" given by Eq. (45).

The shift in θ due to classical radiation damping is [cf. Eq. (27)]

$$\delta\theta_c = \frac{e^5H^3L^2}{3m^4c^8}\,.$$

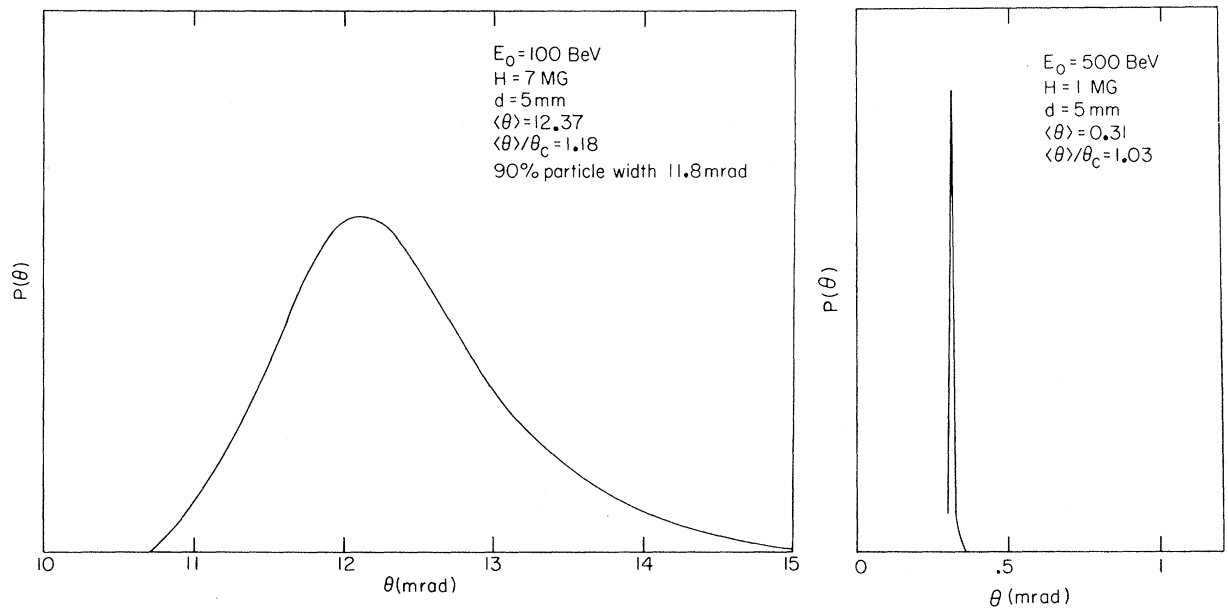

FIG. 9. Deflection of electrons by the magnetic field. $\theta_c = \theta_0 + \delta\theta_c$ is the classical deflection angle including radiation damping [cf. Eq. (26) and Eq. (27)]. $\langle\theta\rangle$ is the expected quantum mechanical deflection angle (obtained by averaging over the distribution). The ratio $\langle\theta\rangle/\theta_c$ indicates the magnitude of the quantum corrections other than the spread.

The modification of the shift due to the quantum corrections to the energy loss rate is

$$\delta\theta_q \cong -(4R_q - 21R_q^2)\delta\theta_c$$
$$= -2.7\times10^{-4}HE(1-\tfrac{21}{4}R_q)\delta\theta_c\,. \quad (47)$$

The modification due to the fluctuation of the center of orbit (the betatron effect) is

$$\Delta\theta_S = -\frac{55}{216\sqrt{3}}\,\alpha R_q^2(L/\lambda\!\!\!^{-})(H/H_q)\delta\theta_c$$
$$= -8\times10^{-10}H^3E^2L\delta\theta_c\,. \quad (48)$$

The angular spread due to downward cascade transitions between states of different principal quantum numbers is given by Eq. (46)

$$\Delta\theta \cong 3.3\left[\alpha(L/\lambda\!\!\!^{-})(H/H_q)\right]^{-1/2}$$
$$\times\left[1+\frac{2\alpha}{3}\gamma(H/H_q)^2(L/\lambda\!\!\!^{-})\right]^{-1}\delta\theta_c$$
$$= 1.5(LH)^{-1/2}(1+1.3\times10^{-4}H^2L\times E)^{-1}\delta\theta_c\,. \quad (49)$$

It is important to distinguish the straggling effect due to cascade transitions from the fluctuation due to betatron oscillations. The betatron oscillation corresponds to a progressive smearing of the particle projectory because of *radiationless* transitions between levels with different values of S. (Thus the betatron oscillation results in no spread in energy space.) On the other hand, the angular spread due to cascade transitions is caused by the fluctuation of radiation energy losses. The betatron oscillation becomes appreciable at the comparatively low energy $E \geq mc^2(H/H_q)^{-1/4}$ where the straggling becomes significant when the effects of radiation on particle energy are non-negligible, i.e., when $E \to mc^2(H/H_q)^{-1/2}$.

Equations (47)–(49) are the most useful formulas for the magnetic-pulse-electron-beam experiments. Comparison of these three equations shows that the cascade spread dominates other quantum effects and is of the same order of magnitude as the classical radiation reaction deflection in the experiments mentioned above.

We have presented here a detailed calculation of the angular deflection because it is easiest to determine the deflection of electron beams in the megagauss experiments. For astrophysical observations, the change of other observables, such as the energy distribution and the radiation spectrum of the particles, is of more interest. It is obvious that the fluctuation effect tends to retain a portion of electrons in an energy range well above that predicted by Eq. (33); a quantitative calculation, however, is beyond the scope of this paper and will be considered elsewhere.

V. SUMMARY, DISCUSSION, AND APPLICATIONS

In Secs. II, III, and IV we have presented a detailed calculation of strong radiative damping and certain quantum mechanical effects. In this section we shall summarize the formulas, indicate their domains of validity, and consider their applications to an ensemble of electrons.

The complete theory of electrodynamics consists of a hierarchy of theories: exact relativistic quantum electrodynamics, relativistic quan-

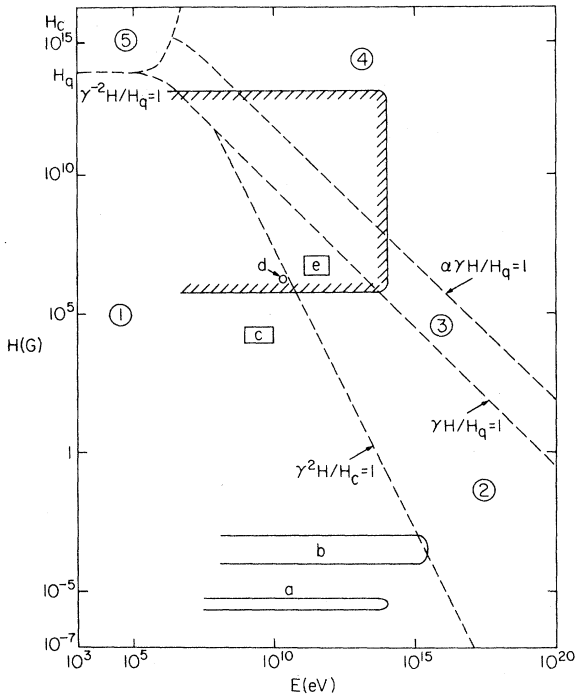

FIG. 10. The range of validity of different levels of synchrotron radiation theory. The basic assumptions and the applicable formulas of each level theory [(1) to (5)] are discussed in Sec. V of the text. This diagram is intended as a crude guide to the applicability of the five levels of electrodynamics theory. One must be aware, however, that sometimes the higher-level effects can be appreciable in the lower-level domain. a, b, c, d, and e represent several astrophysical and experimental situations: (a) Cosmic-ray electrons in the galaxy. (b) Relativistic electrons in Crab nebula (where the radiation spectrum covers a broad range from radio wave to soft γ rays). (c) The existing electron synchrotron. (d) The megagauss experiment using SLAC electron beams. (See Ref. 4.) (e) The megagauss experiment using NAL electron beams. The shadow region represents pulsar electrodynamics which covers all levels of synchrotron theory.

tum electrodynamics with first-order perturbation, classical electrodynamics including radiation reaction, and classical electrodynamics without radiation reaction. The higher-level theory is of course the more general one, but the lower-level theories are usually easier to deal with. Particle energy and field strength are the two parameters determining the applicability of each level of theory. We have therefore constructed a field-strength–particle-energy diagram (Fig. 10) which indicates the validity domains of each level of theory. Several astrophysical as well as laboratory situations are labeled (a, b, c, d, and e) on the diagram.

(I) Region (1): $\gamma^2 H/H_c \ll 1$ ($E^2H \ll 1.5\times10^3$ GeV^2 MG).

Classical electrodynamics valid, radiation reaction negligible. This is the region where the conventional theory of synchrotron radiation applies. The electron is treated as a classical particle whose trajectory is unaffected by radiation loss. The radiation rate is given by

$$\frac{d\gamma}{dt} = -\frac{\gamma^2\omega_H^2}{\omega_0}\sin^2\varphi . \tag{50}$$

The trajectory is a spiral with both the radius of gyration and the pitch angle φ invariant. The components of velocity are

$$v_1(t) = v_0\cos\left(\frac{\omega_H}{\gamma_0}t\right)\sin\varphi_0 ,$$

$$v_2(t) = v_0\sin\left(\frac{\omega_H}{\gamma_0}t\right)\sin\varphi_0 , \tag{51}$$

$$v_3(t) = v_0\cos\varphi_0 .$$

The radiation spectrum is given by

$$\frac{dI}{d\Omega} = \frac{e^2\omega^2}{3\pi^2 c\gamma^2\omega_H^2\sin^2\varphi_0}[A_\parallel^2(\omega) + A_\perp^2(\omega)], \tag{52}$$

$$A_\parallel^2 = (1+\gamma^2\Theta^2)^2 K_{2/3}^2(\omega/\omega_\Theta), \tag{52a}$$

$$A_\perp^2 = (1+\gamma^2\Theta^2)\gamma_0^2\Theta^2 K_{1/3}(\omega/\omega_\Theta), \tag{52b}$$

$$\omega_\Theta = 3(1+\gamma^2\Theta^2)^{-3/2}\gamma^2\omega_H\sin\varphi_0 , \tag{52c}$$

where Θ is the colatitude angle between the observal and the instantaneous orbiting plane.

Polarization of the radiation is

$$\Pi = \frac{K_{2/3}(\omega/\omega_c)}{\int_{\omega/\omega_c}^{\infty} K_{5/3}(x)dx}, \tag{53}$$

where

$$\omega_c = \frac{3\gamma^2\omega_H}{2}\sin\varphi_0 .$$

Equation (52) and Eq. (53) are shown as the dashed curves in Fig. 4 and Fig. 3, respectively. The radiation from a system of particles $N_c(\gamma)$ is given by $\int N_c(\gamma)I(\gamma,\omega)d\gamma$. If, as in most astrophysical cases, the energy spectrum of the electrons can be approximated over a limited energy range by a power law,

$$N_c(\gamma) = N_e\gamma^{-\alpha}, \quad \gamma < \gamma_{\max} ,$$

then the radiation spectrum is approximately

$$I(\omega) \sim \omega^{-(\alpha-1)/2}, \quad \omega \ll \gamma_{\max}^2\omega_H$$
$$\sim 0, \quad \omega \gg \gamma_{\max}^2\omega_H$$

for $\alpha > \frac{1}{3}$. And

$$I(\omega) \sim [1-(\omega/\gamma_{\max}^2\omega_H)^{(1/3-\alpha)/2}]\omega^{1/3}, \quad \omega \ll \gamma_{\max}^2\omega_H$$
$$\sim 0, \quad \omega \gg \gamma_{\max}^2\omega_H \tag{54}$$

for $\alpha < \frac{1}{3}$.

Equations (48)–(54) have been used extensively in the literature.[14] However, one must be aware that in deriving these formulas the electron's energy was assumed constant. It is entirely possible that within the observation time the electron's energy has been reduced significantly even though the energy loss within one revolution is negligible (i.e., $\gamma^2H/H_c \ll 1$). Thus for practical applications the conventional formulas for radiation spectra are further limited by the condition $T/t_{1/2} \ll 1$,[10,11] or

$$EH^2T \ll 3\times10^{-7}\ \text{GeV MG}^2\,\text{sec}, \tag{55}$$

where T is the period of observation and $t_{1/2} = \omega_0/\gamma\omega_H^2$ is the radiation half-life of the electron

For example, in a field $H \sim 1$ MG (pulsar's light cone), the observation period must be shorter than 10^{-6} sec in order for Eq. (50) and Eq. (52) to be applicable. The relevant formulas when $T_{\text{obs}}/t_{1/2} \gtrsim 1$ will be discussed below.

(II) Region (2): $\gamma^2H/H_c > 1$ and $\gamma H/H_q < 1$. ($E^2H > 1.5\times10^3$ GeV^2 MG and $EH < 2.2\times10^4$ GeV MG).

Classical electrodynamics valid, strong radiative damping. In this region the radiation reaction force is stronger than the Lorentz force, and the electron loses a major portion of its energy within one revolution. The trajectory is a fast shrinking spiral [Eq. (7)]. The radiation rate [Eq. (5)] and the instantaneous radiation spectrum [Eq. (A9)] deviate only slightly [to the order of $(\gamma H/H_c)^2$] from the conventional formulas. However, because of the rapid loss of energy, the observed spectrum I_c [Eq. (23)] differs significantly from the conventional one whenever $T/t_{1/2} \gtrsim 1$. For $\gamma^2H/H_c < 1$ (weak radiative damping), we have

$$I_{obs}(\omega)\sim\omega^{1/3}, \qquad \omega<\frac{\omega_0^2}{\omega_H^3T^2}=6\times T^{-2}H^{-3}\ \text{MHz}$$

$$\sim\omega^{-1/2}, \quad \frac{\omega_0^2}{\omega_H^3T^2}<\omega<\gamma^2\omega_H=7\times10^{13}E^2H\ \text{MHz}$$

$$\sim\omega^{1/2}e^{-2\omega/3\gamma^2\omega_H}, \quad \gamma^2\omega_H<\omega \tag{56}$$

with T in sec, H in MG, and E in GeV; i.e., over a large range of frequency the spectrum varies as $\omega^{-1/2}$. For $\gamma^2H/H_c>1$ (strong radiative damping), the spectrum becomes

$$\begin{aligned} I_{obs}(\omega)&\sim\omega^{1/3}, \quad \omega<\omega_0^2/\omega_H^3T^2\\ &\sim\omega^{-1/2},\\ &\quad \omega_0^2/\omega_H^3T^2<\omega<\omega_0/4\pi=1.5\times10^{16}\ \text{MHz}\\ &\sim\omega^{1/3}, \quad \omega_0/4\pi<\omega<\gamma^2\omega_H\\ &\sim\omega^{1/2}e^{-2\omega/3\gamma^2\omega_H}, \quad \gamma^2\omega_H<\omega \end{aligned} \tag{57}$$

i.e., a minimum appears at ~10^{16} MHz due to the damping effect (Fig. 4).

The observed polarization also differs from the conventional value due to the evolutionary effect (Fig. 5).

$$\begin{aligned} \Pi(\omega)&\to0.5, \quad \omega\ll\omega_0^2/\omega_H^3T^2\\ &\approx0.695, \quad \omega_0^2/\omega_H^3T^2\ll\omega\ll4\pi\omega_0\\ &\sim0.5, \quad 4\pi\omega_0\ll\omega\ll\gamma^2\omega_H\\ &\to1, \quad \gamma^2\omega_H\ll\omega. \end{aligned} \tag{58}$$

In astrophysical applications one usually deals with an ensemble of particles. Now that the emitting electrons lose a substantial fraction of their energy within a few revolutions, it is only meaningful to consider radiation from a given injection spectrum $Q(\gamma,t)$ of particles instead of from an equilibrium spectrum. The power emitted from a region where electrons were injected isotropically is given by

$$J(\omega,t)=\int Q(\gamma,t')I_c(\gamma,\omega)d\gamma, \tag{59}$$

where t' is the retarded time. We can classify the time dependence of Q into two extreme cases, one in which the electrons are injected in a burst, and one where the injection rate is constant. The former represents situations where the duration of injection is much shorter than the observation time, and the latter represents a situation where the injection rate hardly varies within the observation time. Let us consider a few representative cases:

(a) Injection of a burst of monoenergetic electrons $Q(\gamma,t)=Q_0\delta(\gamma-\gamma_0)\delta(t-t_0)$. The radiation spectrum would be exactly that of the cumulative spectrum [Eq. (23)] of a single electron with energy γ_0.

(b) Injection of a burst of power-law distribution electrons

$$Q(\gamma,t)=Q_0\gamma^{-\alpha}\delta(t-t_0), \quad \gamma<\gamma_{max}. \tag{60}$$

If, as is often the case in strong radiative damping, the electrons lose most of their energy during observation, the single-particle spectrum may be approximately expressed by

$$\begin{aligned} I_c(\gamma,\omega)&\sim\gamma\omega^{-1/2}, \quad \omega<\gamma^2\omega_H\\ &\sim0, \quad \omega>\gamma^2\omega_H. \end{aligned} \tag{61}$$

The total observed spectrum $J(\omega)$ can be easily evaluated from Eq. (59). For $\alpha>2$

$$\begin{aligned} J(\omega)&\sim\omega^{-(\alpha-1)/2}, \quad \omega\ll\gamma_{max}^2\omega_H\\ &\sim0, \quad \omega\gg\gamma_{max}^2\omega_H. \end{aligned} \tag{62}$$

For $\alpha<2$

$$\begin{aligned} J(\omega)&\sim[1-(\omega/\gamma_{max}^2\omega_H)^{(2-\alpha)/2}]\omega^{-1/2}, \quad \omega\ll\gamma_{max}^2\omega_H\\ &\sim0, \quad \omega\gg\gamma_{max}^2\omega_H. \end{aligned} \tag{63}$$

(c) Continuous injection of monogenergetic electrons which stay in the emitting region for a finite time T_L. In this case T_L must be introduced in order to keep the total number of electrons in the region finite. If T_L is large compared with both the observation time and the radiative life time of the emitting electrons, the observed spectrum $J(\omega)$ is time-independent,

$$\begin{aligned} J(\omega)&=\int Q(\gamma)I_c(\gamma,\omega)d\gamma\\ &=\int N(\gamma)I_I(\gamma,\omega)d\gamma, \end{aligned} \tag{64}$$

where $N(\gamma)$ is the equilibrium distribution satisfying

$$\frac{d}{d\gamma}\left[N(\gamma)\frac{d\gamma}{dt}\right]+\frac{N(\gamma)}{T_L}=Q(\gamma). \tag{65}$$

For $Q(\gamma)=Q_0\delta(\gamma-\gamma_0)$, the steady-state energy spectrum of electrons is

$$\begin{aligned} N(\gamma)&=\frac{\omega_0Q_0}{\omega_H^2}\gamma^{-2}\exp(-\omega_0/\gamma\omega_H^2T_L), \quad \gamma<\gamma_0\\ &=0, \quad \gamma>\gamma_0 \end{aligned} \tag{66}$$

and the total radiation spectrum varies as $J(\omega)\sim\omega^{-1/2}$ within the frequency range $\omega_0^2/\omega_H^3T_L^2<\omega<\gamma_0^2\omega_H$. Outside this range there is little radiation.

(d) Continuous power-law injection $Q=Q_0\gamma^{-\alpha}$. In this case the steady-state spectrum for $\alpha>1$

$$N(\gamma) = TQ_0\gamma^{-\alpha}, \quad \gamma < \omega_0/\omega_H{}^2T$$
$$= \frac{\omega_0 Q_0}{(\alpha-1)\omega_H{}^2}\gamma^{-(\alpha+1)}, \quad \gamma > \omega_0/\omega_H{}^2T \qquad (67)$$

and the radiation spectrum

$$J(\omega) \sim \omega^{-(\alpha-1)/2}, \quad \omega \ll \omega_0{}^2/\omega_H{}^3T_L{}^2$$
$$\sim \omega^{-\alpha/2}, \quad \omega \gg \omega_0{}^2/\omega_H{}^3T_L{}^2, \qquad (68)$$

i.e., the spectrum steepens by a half power at $\omega_c = 6\times10^6 T_L{}^{-2}H^{-3}$ MHz.[23,24] For $\alpha < 1$ we have

$$N(\gamma) = TQ_0\gamma^{-\alpha}, \quad \gamma < \omega_0/\omega_H{}^2T$$
$$= \frac{\omega_0 Q_0}{(1-\alpha)\omega_H{}^2}\gamma_{\max}{}^{(1-\alpha)}[1-(\gamma/\gamma_{\max})^{(1-\alpha)}]\gamma^{-2},$$
$$\omega_0/\omega_H{}^2T_L < \gamma < \gamma_{\max} \qquad (69)$$

and the radiation

$$J(\omega) \sim \omega^{-(\alpha-1)/2}, \quad \omega \ll \omega_0{}^2/\omega_H{}^3T_L{}^2$$
$$J(\omega) \sim \omega^{-1/2}, \quad \omega_0{}^2/\omega_H{}^3T_L{}^2 \ll \omega \ll \gamma_{\max}{}^2\omega_H \qquad (70)$$

i.e., a break of more than a half power at ω_c.

In the above discussions we have neglected the quantum corrections, which become significant when $R_q = \gamma H/H_q \to 1$. However, the fractional energy carried away by the synchrotron photon is $\sim R_q/(1+R_q)$, if $R_q/(1+R_q)$ is not negligibly small. Then the statistical fluctuations which are inherent in the quantum transitions could be appreciable even when the inequality $\gamma H/H_q < 1$ is fullfilled. We shall discuss this effect in the next paragraph.

(III) Region (3): $\gamma H/H_q > 1$ but $\alpha\gamma H/H_q < 1$ ($EH > 2.2\times10^4$ GeV MG but $EH < 3\times10^6$ GeV MG).

In this region the energy carried away by the synchrotron photons becomes comparable to the energy of the emitting electron. Thus although the electron itself is still a well-localized classical particle, the radiation process must be calculated quantum mechanically. Because $\alpha\gamma H/H_q < 1$, the radiative corrections are small and the first-order pertubation theory is valid in this region.

The radiation rate is given by Eq. (33), it is smaller than the corresponding classical radiation rate. The instantaneous radiation spectrum is similar to the classical one at low frequency, but cut off in the high frequency limit at $\omega = \gamma^2\omega_H/(1+R_q)$. The inward spiraling of the particle orbit is slower than that predicted by the classical formula because the radiation rate is less. Here, however, one must take the quantum fluctuation into consideration. Instead of a smoothly shrinking spiral, the electron moves like a Brownian particle with successively smaller radius of curvature. As for the radiation spectrum, if during observation the electron makes a number of successive downward transitions, the observed spectrum includes photons emitted from all transitions. Because of the inherent statistical nature of quantum transitions, one cannot predetermine the subsequent states of an electron undergoing cascade transitions. Therefore in the calculation of the cumulative spectrum, the effect of quantum broadening must be included. A few examples have been worked out numerically. (See Ref. 20.) For $T_{\text{obs}} \gg t_{1/2}$, the quantum mechanical cumulative spectrum has the same characteristics as the classical one except that (i) the quantum mechanical spectrum breaks off at the frequency $\gamma_0{}^2\omega_H/(1+R_q)$, and (ii) the dip at $\gamma^2\omega_H/(1+4\pi R_0)$ is flattened somewhat, because it is now possible that the first few quantum transitions would only emit (relatively) soft photons to leave the electron in an energy level near the initial state, where classically the electrons energy must be reduced to $\gamma_0/(1+4\pi R_0)$ after one revolution. Therefore, the over-all radiation spectrum of a stream of mono-energetic electrons injected into an emission region would be $\sim\omega^{1/2}$ with a cutoff at $\gamma^2\omega_H/(1+R_q)$. In cases where an equilibrium spectrum of electrons $N(\gamma)$ exists and $\gamma H/H_q > 1$ over the energy range of interest, the radiation spectrum of $N(\gamma)$ is simply $J(\omega) = \int_{\hbar\omega/mc^2} N(\gamma)d\gamma$, for now the instantaneous spectrum for a single electron is roughly constant up to a maximum frequency $\omega = \gamma mc^2/\hbar$. For a power law distribution $N(\gamma) \sim \gamma^{-\alpha}$, one has

$$J(\omega) \propto \omega^{-\alpha+1},$$

where for a Maxwellian $N(\gamma) \sim e^{-\gamma mc^2/kT}$

$$J(\omega) \propto e^{-\hbar\omega/kT}.$$

These spectra are similar to the ordinary bremsstrahlung spectra.

(IV) Region (4): $\alpha\gamma H/H_q > 1$ ($EH > 3\times10^6$ GeV MG).

In this region the external field measured in the electron's rest frame becomes larger than the intrinsic self-field $e^2/r_0{}^2$ ($r_0 = e^2/mc^2$). The electrodynamic interaction becomes "strong" and the e^2 expansion used in the first-order pertubation theory of quantum electrodynamics breaks down. Although at present this region belongs to the never-never land in laboratory physics, in certain astrophysical cases (such as the pulsar magnetosphere), the parameters are such that the effect of strong radiation corrections must be considered. In order to have a crude guide in astrophysical application, a calculation aimed at an order of magnitude estimation on the various high-order terms is now under way by White.[25] It is of interest to mention that the modification to the classical instantaneous radiation rate is proportional to $(R_0/$

$\gamma)^2$ (Eq. 5). Since the effect of energy damping cannot reflect on the instantaneous quantities, this deviation must be due to the modification of the radiation process caused by reaction forces, i.e., due to the "correction" part of the radiation reactions. Note that since $R_c/\gamma \equiv \frac{4}{9}\alpha R_q$, the classical results are consistent with the quantum electrodynamical results at least to the lowest order of radiative corrections.

(V) Region (5): $H/\gamma^2 H_q \sim 1$ ($HE^{-2} \sim 1.8\times 10^{14}$ MG GeV^{-2}).

Here the de Broglie wavelengths of the electron become comparable to the Larmor radius, and the energy levels (Landau level) characterizing the perpendicular motion of the electron become distinctly discrete. The level spacing between two levels is

$$mc^2[(1+2N_1H/H_q)^{1/2} - (1+2N_2H/H_q)^{1/2}].$$

If the energy of the particle is $\gamma < (1+2H/H_q)^{1/2}$, then the particle will stay in the ground state and stream along the field line emitting no synchrotron radiation. If the energy of the particle is $\gamma > (1+2H/H_q)^{1/2}$, then transitions between two Landau levels give discrete spectral lines. Chiu and Canuto had published a series of articles discussing the radiation mechanisms in this region.[26]

ACKNOWLEDGMENT

I wish to thank Dr. T. Erber for several useful discussions. I also want to thank Dr. S. L. O'Dell and L. Sartori for pointing out a few minor errors involving terms of order $(R_0/\gamma_0)^2$ in my earlier article published in Phys. Rev. Letters. These errors are corrected in the present article.

APPENDIX

The radiation emitted by an accelerated relativistic charge is beamed into a narrow cone in the direction of the velocity vector. A distant observer located in the orbiting plane sees a short pulse of radiation as the searchlight beam sweeps across the observation point. The intensity distribution of this pulse is related to the motion of the particle at the instant of emission.

$$\frac{dI(\omega)}{d\Omega} = \frac{e^2\omega^2}{4\pi^2 c^3}\left|\int_{-\infty}^{\infty} \vec{n}\times(\vec{n}\times\vec{v})e^{i\omega(t-\vec{n}\cdot\vec{r}/c)}dt\right|^2 . \quad \text{(A1)}$$

The integration is over the retarded time of the radiating particle.

For an electron deflected by a magnetic field, the duration of the pulse at emission is $\sim\omega_H^{-1}$ [it shortens to $(\gamma^2\omega_H)^{-1}$ at observation due to the retardation effect]. Thus we can expand v_1, v_2, and r_1 from Eq. (7) in powers of $1/\gamma_0$, R_0/γ_0, and $\omega_H t/\gamma_0$.[27]

$$v_1 = v_0\left(1 - \frac{R_0}{\gamma_0^3}\omega_H t - \frac{1}{2\gamma_0^2}\omega_H^2 t^2 - \frac{R_0}{2\gamma_0^3}\omega_H^3 t^3\right), \quad \text{(A2)}$$

$$v_2 = v_0\left[\frac{\omega_H t}{\gamma_0} + \frac{R_0}{2\gamma_0^2}(\omega_H t)^2 + O\left(\frac{1}{\gamma_0^3}\right)\right], \quad \text{(A3)}$$

$$r_1 = v_0 t\left(1 - \frac{R_0}{2\gamma_0^3}\omega_H t - \frac{1}{6\gamma_0^2}\omega_H^2 t^2 - \frac{R_0}{8\gamma_0^3}\omega_H^3 t^3\right). \quad \text{(A4)}$$

Substituting into (A1), we have

$$\omega(t - \vec{n}\cdot\vec{r}/c) \approx \frac{3}{2}\frac{\omega}{\omega_\Theta}(x + \tfrac{1}{3}x^3 + \alpha_1 x^2 + \alpha_2 x^4), \quad \text{(A5)}$$

$$\vec{n}\times(\vec{n}\times\vec{\beta}) \simeq \frac{1}{c}(\vec{e}_\perp v_1 \sin\Theta - \vec{e}_\parallel v_2)$$

$$\simeq \Theta\vec{e}_\perp - \left[\frac{\omega_H t}{\gamma_0} + \frac{R_0}{2}\left(\frac{\omega_H t}{\gamma}\right)^2\right]\vec{e}_\parallel , \quad \text{(A6)}$$

where $x = \omega_H t(1+\gamma^2\Theta^2)^{1/2}$, $\omega_\Theta = 3(1+\gamma^2\Theta^2)^{-3/2}\gamma_0^2\omega_H$, Θ is the colatitude angle, $\vec{e}_\perp$ and $\vec{e}_\parallel$ denote the two polarization vectors, and $\alpha_1 x^2$ and $\alpha_2 x^4$ are the two terms introduced by the radiation damping

$$\alpha_1 = \frac{R_0}{\gamma_0}(1+\gamma_0^2\Theta^2)^{-1/2}, \quad \text{(A7)}$$

$$\alpha_2 = \frac{R_0}{4\gamma_0}(1+\gamma_0^2\Theta^2)^{1/2}. \quad \text{(A8)}$$

The radiation spectrum becomes

$$\frac{dI(\omega)}{d\Omega} = \frac{e^2\omega^2}{4\pi^2 c^3}(A_\parallel^2 + A_\perp^2), \quad \text{(A9)}$$

where

$$A_\parallel = A_\parallel^a + \Delta A_\parallel , \quad \text{(A10)}$$

$$A_\parallel^a = \frac{1+\gamma^2\Theta^2}{\omega_H\gamma} \times \int_{-\infty}^{\infty} x\exp\left[i\frac{3\omega}{2\omega_\Theta}(x + \tfrac{1}{3}x^3 + \alpha_1 x^2 + \alpha_2 x^4)\right]dx, \quad \text{(A11)}$$

$$\Delta A_\parallel = \frac{R_0}{2\gamma}\frac{(1+\gamma^2\Theta^2)^{3/2}}{\gamma\omega_H} \times \int_{-\infty}^{\infty} x^2\exp\left[i\frac{3\omega}{2\omega_\Theta}(x + \tfrac{1}{3}x^3 + \alpha_1 x^2 + \alpha_2 x^4)\right]dx, \quad \text{(A12)}$$

$$A_\perp = \frac{\Theta(1+\gamma^2\Theta^2)^{1/2}}{\omega_H} \times \int_{-\infty}^{\infty} \exp\left[i\frac{3\omega}{2\omega_\Theta}(x + \tfrac{1}{3}x^3 + \alpha_1 x^2 + \alpha_2 x^4)\right]dx. \quad \text{(A13)}$$

$A_{\parallel}^{q}$ and $A_{\perp}$ deviate from the unperturbed synchrotron spectrum by the terms $\alpha_1 x^2$ and $\alpha_2 x^4$ in the exponent. The term $\alpha_2 x^4$ becomes comparable to other terms in the exponent when $x \sim \alpha_2^{-1/3}$, but then the argument $x + \frac{1}{3}x^3 + \alpha_1 x^2 + \alpha_2 x^4 \sim \gamma_0^3$ and the integrand oscillates rapidly unless $\omega \lesssim \omega_H/\gamma$, which is beyond the range of validity of the present analysis. Therefore $\alpha_2 x^4$ can be neglected in the exponent. The term $\alpha_1 x^2$ may be transformed away by changing ω_Θ to $\omega_\Theta/(1-\alpha_1^2)^{3/2}$. To estimate the contribution from $\Delta A_{\parallel}$, we observed that the integral

$$\int_{-\infty}^{\infty} x^2 \exp\left[i\frac{3\omega}{2\omega_\Theta}\left(x+\tfrac{1}{3}x^3\right)\right] dx = 2\int_0^{\infty} x^2 \cos\left[\frac{3\omega}{2\omega_\Theta}\left(x+\tfrac{1}{3}x^3\right)\right] dx$$

$$= 2\int_0^{\infty} \cos\left(\frac{3\omega}{2\omega_\Theta} y\right) dy - \int_0^{\infty} \cos\frac{3\omega}{2\omega_\Theta}\left(x+\tfrac{1}{3}x^3\right) dx = \delta\left(\frac{3\omega}{2\omega_\Theta}\right) - \frac{2}{\sqrt{3}} K_{1/3}\left(\frac{\omega}{\omega_\Theta}\right) . \tag{A14}$$

Thus, the over-all modification of the instantaneous spectrum by the radiation reaction effect is to increase the critical frequency by a factor of $(1-\alpha^2)^{-3/2}$ and to increase slightly the radiation intensity polarized in the plane of the orbit. All these corrections are of the order of $R_0/\gamma_0 \ll 1$.

---

*Work supported in part by Purdue Research Foundation.

[1]For a comprehensive review, see F. Rohrlich, *Classical Charged Particles* (Addison-Wesley, Reading, Mass., 1962).

[2]T. Erber, Fortschr. Physik 9, 343 (1961).

[3]It should be noted that Eq. (1) deals with the dynamics of a point particle but not its structure. The divergent self-energy term is ignored by lumping the electromagnetic mass together with the bare mass to yield the finite observed mass.

[4]F. Herlach, R. McBroom, T. Erber, J. J. Murray, and R. Gearhart, in Proceedings of Particle Accelerator Conference, Chicago, 1971 (unpublished).

[5]F. Herlach, Rep. Progr. Phys. 31, 341 (1968).

[6]C. M. Fowler, W. B. Garn, and R. S. Caird, J. Appl. Phys. 31, 588 (1960).

[7]G. N. Plass, Rev. Mod. Phys. 33, 37 (1961).

[8]A. A. Sokolov, N. P. Klepikov, and I. M. Ternov, Sov. Phys. JETP 23, 632 (1952); J. Schwinger, Proc. Nat. Acad. Sci. U. S. 40, 132 (1954).

[9]See W. Heitler, in *The Quantum Theory of Radiation* (Oxford Univ. Press, Oxford, Eng., 1954). The nomenclatures "radiation damping" and "radiative correction" are also taken from Heitler's book.

[10]C. S. Shen, Phys. Rev. Letters 24, 410 (1970).

[11]N. D. Sen Gupta, Phys. Letters 32A, 103 (1970); C. S. Shen, *ibid.* 33A, 322 (1970).

[12]N. D. Sen Gupta, Int. J. Theor. Phys. 4, 389 (1971); Phys. Rev. D 5, 1546 (1972).

[13]J. D. Jackson, *Classical Electrodynamics* (Wiley, New York, 1962).

[14]For a more detailed discussion on synchrotron emission and its application to astrophysics, see V. L. Ginzburg and S. I. Syrovatskii, Annu. Rev. Astron. Astrophys. 3, 297 (1965).

[15]V. L. Ginzburg and S. I. Syrovatskii, Annu. Rev. Astron. Astrophys. 7, 375 (1969).

[16]A comprehensive discussion on possible experimental studies of electromagnetic conversion processes in intense magnetic field is given by T. Erber, Acta Phys. Austr., Suppl. VIII, 323 (1971).

[17]For a detailed report on the setup and the results of the IIT-SLAC experiment, see R. C. McBroom, M. S. thesis, 1971 (unpublished).

[18]For a detailed discussion on quantum theory of synchrotron emission see A. A. Sokolov and I. M. Ternov, *Synchrotron Radiation* (Pergamon, New York, 1968), and T. Erber, Rev. Mod. Phys. 38, 626 (1966).

[19]Actually, at $R_q \gg 1$ the amplitude of the second-order term increases as $\alpha R_q^{2/3}$ and the fourth-order term increases as $\alpha R_q \ln R_q$. See V. I. Ritus, Ann. Phys. (N.Y.) 69, 555 (1972).

[20]C. S. Shen and D. White, Phys. Rev. Letters 28, 455 (1972).

[21]P. Urban and K. Wittmann, Acta Phys. Austr. (to be published).

[22]This method is described in detail in D. White, Phys. Rev. D 5, 1930 (1972).

[23]D. F. Falla and A. Evans, in AU Symp. No. 46, 1971 (unpublished).

[24]The steepening of radiation as well as particle spectrum due to leakage-radiation competition is a well-known fact in the problem of cosmic-ray propagation. Recently J. Jaffe and A. Treves [Astrophys. Letters 9, 39 (1971)] have considered its significance in the high-energy radiation from Crab pulsar.

[25]D. White, Ph.D. thesis, Purdue University (unpublished).

[26]V. Canuto and H. Y. Chiu, Space Sci. Rev. 12, 3 (1971).

[27]We have assumed the time spent by the particle in the magnetic field to be much longer than ω_H^{-1}.